Dalton Transactions

Accepted Manuscript

ROYAL SOCIETY OF CHEMISTRY

www.rsc.org/dalton

Journal Name

RSCPublishing

ARTICLE

Anion complexation with cyanobenzoyl substituted first and second generation tripodal amide receptors: crystal structures and solution studies

Md. Najbul Hoque, Abhijit Gogoi and Gopal Das*

Cite this: DOI: 10.1039/x0xx00000x

Received 00th January 2012,
Accepted 00th January 2012

DOI: 10.1039/x0xx00000x

www.rsc.org/

Anion complexation properties of two new tripodal amide receptors have been extensively studied here. Two tripodal receptors have been synthesized from the reaction of cyanobenzoyl acid chloride with two tri-amine building blocks such as (i) tris(2-aminoethyl)amine and (ii) tris(2-(4-aminopheoxy)ethyl)amine which resulted the first ($\mathbf{L_1}$) and second ($\mathbf{L_2}$) generation tripodal amide respectively. Details comparison of coordination behavior with anions is also described by crystallographic and solution state experiment. Crystal structure demonstrates various type spatial orientations of tripodal arms in two receptors and concomitantly interacts with anions distinctively. Intramolecular H-bonding between amide N−H and C=O prevent opening of the receptor cavity in the crystal which lead to locked conformation of $\mathbf{L_1}$ having C_{3v} symmetry and makes amide hydrogen unavailable for anion which results side cleft anion binding. Whereas in $\mathbf{L_2}$ we conveniently shift the anion binding sites to distant position which increases cavity size as well as ruled out any intramolecular H-bonding between (amide N−H and C=O. Crystal structure shows a different orientation of arms in $\mathbf{L_2}$, it adopts a quasi-planar arrangement with C_{2v} symmetry. In the crystal structure two arms pointed in the same direction and while extending the contact the third arm is H-bonded with the apical N-atom through –CN group making a pseudo capsular cavity where anion interacts. Most importantly spatial reorientation of the receptor $\mathbf{L_2}$ from C_{2v} symmetry to folded conformation with C_{3v} symmetry was observed only in the presence of octahedral SiF_6^{2-} anion and form sandwich type complex. Receptors $\mathbf{L_1}$ and $\mathbf{L_2}$ are explored toward their solution state anion binding abilities. The substantial changes in chemical shifts were observed for the amide (–NH) and aromatic hydrogen (–CH) (especially for F^-) indicating the role of these hydrogen in anion binding. Anion interacts with receptor $\mathbf{L_2}$ more strongly than $\mathbf{L_1}$ as confirmed by ^{1}H NMR titration upon monitoring the –NH signal.

Introduction

Anions are vital species and have widespread use in environmental, biological processes and molecular recognition studies.[1-6] Various artificial systems have been reported to achieve selective molecular recognition and sensing of anions and these system provides a fascinating control in formation of supramolecular assemblies.[7-9] Recognition of anionic species is accomplished by electrostatic and H-bonding interactions.[10-14] Additionally recent advances also shows chemical reactions are also very promising for anion recognition.[15-19] Since beginning of supramolecular chemistry, tris(2-aminoethyl)-amine (tren) is effectively used as a primary building block along with amine, amide and urea functions for variety of anion recognition with high level of satisfaction.[20] Nature often recognizes anion, functionalized with amide as H-bond donors. Therefore, a variety of molecular receptors have been developed containing amide platform that perform recognition of anionic targets by establishing a complementary H-bonds.[21-23] Few amide base receptors containing tren as building block recognize anions through side cleft or capsular binding.[24] Anion complexation and anion induced supramolecular assembly is more challenging as H-bonds formed by anions are weaker that are strongly influenced by external stimuli like pH, nature of guest and solvent.[25] When anions are an inevitable part of supramolecular aggregates, by proper tuning the assembly and disassembly processes can be explored nicely. So it was anticipated that if the anion is changed with other anions it might collapse or re-orient the assembly. Therefore, by varying the geometry of the anions involved in a self-assembly process, it should in principle be possible to re-orient or rupture the self-

assembled architectures to form a completely new assembled system.

Very promising result reported by P. Ghosh *et.al* shows orientation of all six arms of benzene capped hexa-amide in presence of fluoride forming a dimeric capsular complex.[26] The most astonishing fact is that in presence of acetate ion the conformation of the receptor changed completely and resulted a non-capsular assembly. Most recently, we have reported the anion induced conformational changes of a cresol-based tripodal receptor.[27] We are infancy at this stage to know more about the fascinating structure directing role of anion. In continuation of our work on solid state anion recognitions,[28-40] here we have synthesized cyanobenzoyl substituted flexible tripodal amides which includes first generation receptor (**L_1**) where tren is used as a simple building block and elongated second generation tripodal (**L_2**) where tri-amine of a tripodal is used as a building block. Two receptors having characteristic length and cavity, elegantly exploited for anion complexation and anion binding studies were also carried out in solid and solution state. We also examined the dimensionality and nature of the anions play a crucial role in making various molecular interactions possible in complexation of various anions in both receptors. Most importantly we have noticed that the self-alignment and orientation of the flexible second generation tripodal is greatly influenced by the size and shape of the anion. The X-ray structure shows **L_1** is internally locked and could not welcome anions into its C_{3v} symmetric cavity, shows side cleft anions binding. Positioning of amide functionality to a distant position with respect to apical N-atom results a bigger cavity and subsequently intimidate the N−H···O=C intramolecular H-bond unlike in **L_1**. The receptor form quasi-planar arrangement of the arms, with two arms close each other while third arm pointing to opposite direction giving pseudo capsular complex during H-bonding interaction. Finally we could able to compare the recognition of anionic guests of different shapes/geometry and solid state organization of the two kind of receptor of varying podal length. Interestingly anion induced reorientation of the receptor **L_2** was observed during recognition of octahedral SiF_6^{2-} anion. In the solid state –CN group provide further stabilization to the supramolecular complexes through C–H···π and anion···π interactions. Moreover the solution state interaction phenomena of two receptors in neutral form with the anions of various shape and size like spherical (F^-, Br^-, I^-), planner (NO_3^-), tetrahedral (ClO_4^-) and octahedral (SiF_6^{2-}) by detailed ^{1}H NMR studies along with their molecular binding was thoroughly analyzed.

Results and discussion

The sequential synthesis of 4-cyanobenzoyl substituted first and second generation tripodal amide receptors (**L_1** and **L_2**) and their anion complexation have been studied systematically. Our notion in designing the receptors containing cyano group is as follows. The strength of an aromatic C–H donor (effective anion binding group) can be enhanced through the addition of different functional groups on parent phenyl ring. It has been well established that the electron-withdrawing substituent on the benzene ring assist the active participation of the aromatic –CH protons toward anion binding *via* C–H···anion interactions. The –CN group is known to act as strong electron withdrawing substituent and therefore we have introduced cyano-substituted phenyl terminals to improve the anion binding affinities. The amide based tripodal receptors rarely forms capsular complex. Being inspired from our previous report of capsular assembly of tripodal amine[30,31] and versatile anion coordination of its elongated derivatives,[32,33] herein we have attempted to get capsular complex through various modifications like (i) changing the substituents (ii) creating larger cavity suitable for guest inclusion by elongating of the receptor's arm. This is our second report of tripodal amide (**L_2**) in this category and given our interest in main group anions, we decided further examinations to achieve the goal with this receptor. Additionally we have opportunity to examine the effect of arm length towards anion coordination. With the deliberate incorporation of a phenyl subunit, **L_2** are able of creating a specific spatial arrangement of arms compared to **L_1** which would significantly alter the anion binding fashion. Moreover anion induced dramatic folding and unfolding of the elongated receptor **L_2** is also important outcome of the study.

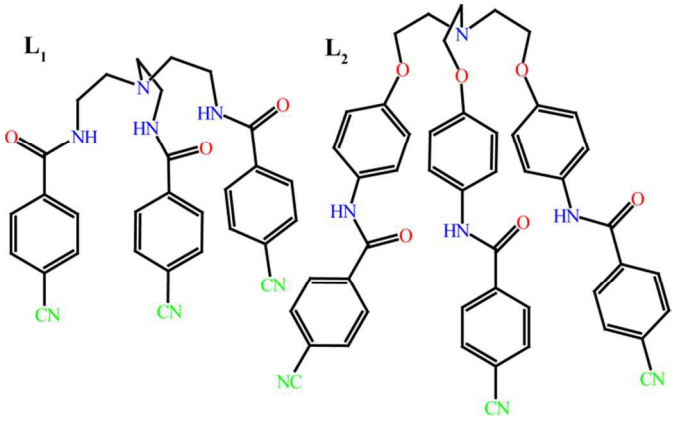

Scheme 1 Molecular structure of the first and second generation tripodal amide receptors **L_1** and **L_2** respectively.

Crystal structure studies

Anion complexation studies in solid state with first and second generation tripodal amides

First generation tripodal amide L_1 and its anion complexation

The receptor **L_1** crystallizes in monoclinic space group C2/*c* (Table S1). The receptor contains C_{3v} symmetry and carbonyl group has tendency to stay outwards from the cavity. Among three amide oxygen, O3 of one arm acts as an acceptor and is involved in strong intramolecular H-bonding interaction with the donor amide hydrogen H2N which possibly holds the arms together. While amide oxygen O1 is H-bonded with amide hydrogen H3N and ortho aromatic hydrogen H15 in a fashion which lead to the formation of centrosymmetric dimer (Fig. S1b). The amide oxygen O2 interacts with H4N of the

neighboring receptor which along with C−H···π interactions finally resulted 1-D assembly of the receptor where they are arranged in up and down fashion (Fig. S1c). All three amide oxygens form bifurcated H-bonds either with NH or aromatic CH. The average N−H···O and C−H···O distances are 2.976 Å and 3.367 Å which are fairly comparable to previously reported values.[24] Very interestingly two −CN groups (N5 and N7) involved in C_{ar}–H···N H-bond with aromatic hydrogen as well as C_{ar}–H···π by virtue of π-cloud of the −CN group (Fig. S1d).

The tripodal receptor $\mathbf{L_1}$ is enriched with H-bond functionalities which enable us to study anion coordination with anionic guests of different size and geometry. Anion complexation studies in acidic condition with protonated receptor will be discussed here. With spherical Br^- ion, we prepared complex **[HL_1·Br] (2)**. The complex **2** crystallizes in the triclinic space group *P1̄*. Protonated apical N-atom form strong H-bond (N1···O1 = 2.750(3) Å) with one of amide C=O, which is now pointed inwards of the C_{3v} cavity of the receptor. The *endo* oriented amide C=O also form a strong intramolecular H-bonding with amide hydrogen H4N (N4···O1 = 2.878(3) Å). Other two *exo*-oriented O2 and O3 interact with phenyl hydrogen H17 and H15, H3N of next receptors (Fig. S2a). Though two amide hydrogen are pointed towards C_{3v} symmetric cavity, Br^- ion could not be encapsulated due to the strong intramoleular H-bonds which did not allow the receptor to open to well come bromide ion. Thus, it remains outside the

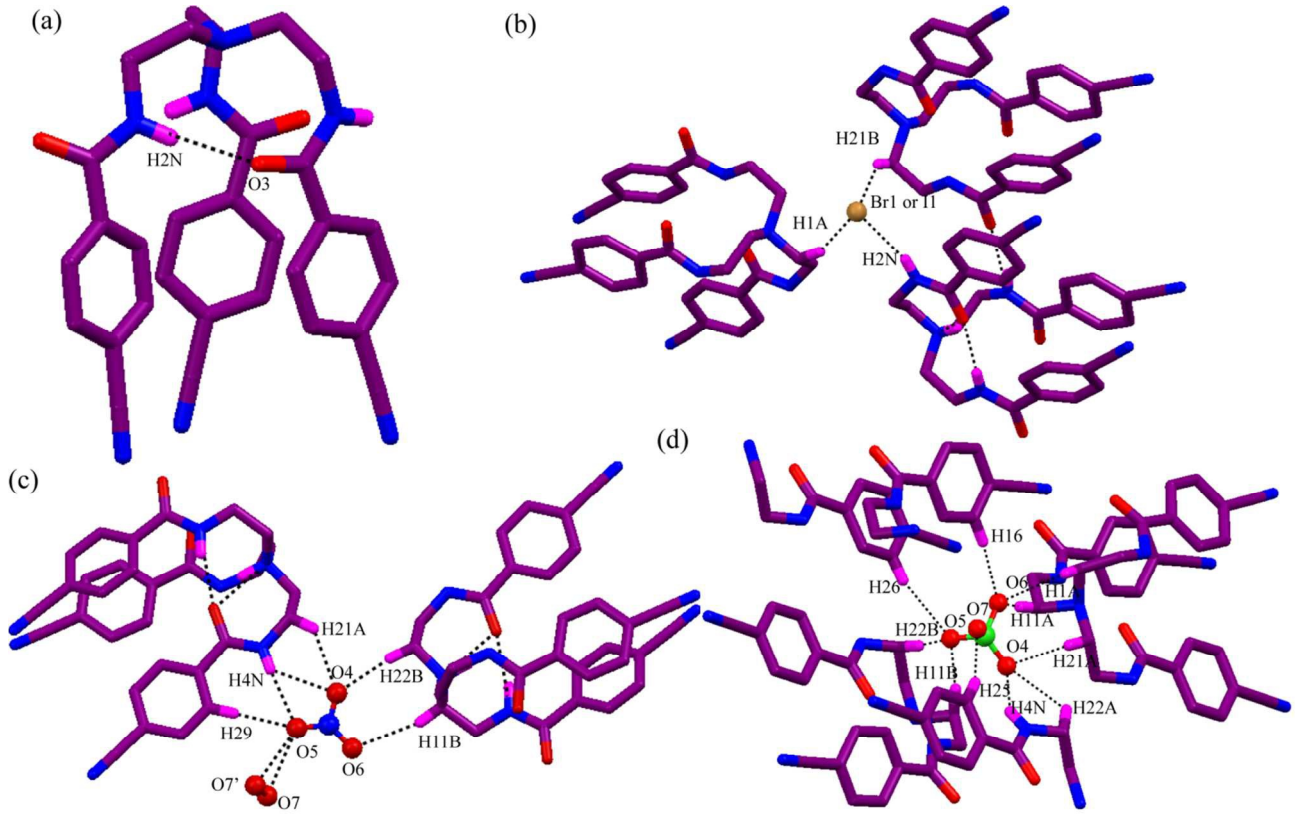

Fig. 1 (a) Conformationally locked orientation of $\mathbf{L_1}$. (b) Close-up view of H-bonding interactions with bromide/iodide ion in complex **[L_1H·Br](2)** and **[HL_1·I](3)**. (c) Simplified sketch of the seven coordinated NO_3^- ion in complex **[$(L_1H)_2$·2NO_3·H_2O](4)**. (d) Illustration of H-bonding around ClO_4^- anion in complex **[L_1H·ClO_4](5)** with five encircling $\mathbf{L_1H^+}$ receptors.

cavity and is surrounded by three $\mathbf{L_1H^+}$ receptors (Fig. 1b) through one N–H···Br^- interactions and two C–H···Br^- interactions. The tri-coordinated Br^- ion lies outside of the hydrogen bond donor plane H2N, H1A and H21B. Packing along *b*-axis depicted the formation of layers which are connected through –CN and aromatic CH hydrogen (Fig. S2b). The presence of Br^- ion inevitably disrupts the formation dimeric interaction between receptors as observed in case of free receptor. As a course of anion-receptor interaction, we have also isolated isostructural iodide complex **[HL_1·I](3)** of the receptor. The bigger iodide anion behaves very similarly as bromide ion. The crystal structure analysis shows that the inter and intramolecular interactions patterns are exactly similar to that of complex **2**. The conformation of the protonated receptor and coordination environment around I^- ion is also similar to complex **2**. The tri-coordinated geometry of halide ion is observed by previously reported tripodal triamide.[11] The details contact distances and angles are given in Table 1.

The interaction of the receptor with oxyanion like planar (nitrate) and tetrahedral (perchlorate) were also studied. Both the nitrate **[$(L_1H)_2$·2NO_3·H_2O](4)** and perchlorate **[L_1H·ClO_4](5)** complexes crystallizes in triclinic system. The conformation of the receptor in these cases are similar and interaction pattern of amide NH and C=O is also retained like the halide complexes. Therefore the protonated receptor interacts with nitrate and perchlorate anion in these complexes

Table 1. Non-covalent contacts in $\mathbf{L_1}$ and its anion complexes.

D–H···A	d(D···A)/Å	d(H···A)/Å	∠(D–H–A)/º
L_1			
N2–H2N···O3	3.00(2)	2.14(1)	160.0(9)
N3–H3N···O1	3.00(2)	2.12(1)	165.0(1)
N4–H4N···O2	3.012(2)	2.23(1)	151.0(9)
C15–H15···O1	3.200(2)	2.276(1)	173.0(1)
C28–H28···O3	3.346(2)	2.668(1)	130.3(1)
C25–H25···O2	3.557(2)	2.707(1)	152.3(1)
[L_1H·Br](2)			
N1–H1N···O1	2.750(3)	2.00(2)	141.0(2)
N2–H2N···Br1	3.343(3)	2.51(3)	158.0(2)
N3–H3N···O3	2.881(3)	2.09(2)	159.0(2)
N4–H4N···O1	2.878(3)	2.10(3)	156.0(3)
C1–H1A···Br1	3.895(3)	3.00(4)	155.0(2)
C21–H21B···Br1	3.711(2)	3.00(4)	142.0(1)
[L_1H·I](3)			
N1–H1N···O1	2.739(8)	2.00(8)	141.0(2)
N2–H2N···I1	3.569(6)	2.78(6)	158.0(2)
N3–H3N···O3	2.858(7)	2.08(5)	159.0(2)
N4–H4N···O1	2.863(7)	2.06(5)	156.0(3)
C1–H1A···I1	4.069(7)	3.16(6)	157.0(4)
C21–H21A···I1	3.886(6)	3.05(5)	145.0(4)
[(L_1H)$_2$·2NO$_3$·H$_2$O](4)			
N1–H1N···O3	2.73(4)	1.770(4)	139.0(3)
N2–H2N···O2	2.89(4)	2.110(4)	154.0(3)
N3–H3N···O3	2.88(4)	2.17(3)	149.0(3)
C21–H21A···O4	3.159(7)	2.433(5)	131.3(3)
C22–H22B···O4	3.241(8)	2.276(7)	172.7(3)
O7w···O5	2.880(2)	---	---
O7w···O5	2.770(2)	---	---
N4–H4N···O5	3.080(8)	2.220(4)	158.0(4)
C29–H29···O5	3.255(9)	2.378(8)	157.0(3)
C11–H11B···O6	2.693(7)	3.637(7)	164.6(2)
[L_1H·ClO$_4$](5)			
N1–H1N···O3	2.73(4)	1.980(4)	147.0(3)
N2–H2N···O2	2.88(4)	2.10(3)	151.0(2)
N3–H3N···O3	2.87(4)	2.08(2)	152.0(2)
N4–H4N···O4	3.04(7)	2.35(7)	137.0(2)
C21–H21A···O4	3.537(9)	2.588(7)	166.0(3)
C11–H11B···O5	3.438(8)	2.516(7)	158.6(3)
C22–H22B···O5	3.369(7)	2.439(6)	160.4(3)
C26–H26···O5	3.507(8)	2.603(7)	164.5(3)
C1–H1A···O6	3.478(8)	2.671(7)	141.0(3)
C11–H11A···O6	3.515(7)	2.639(6)	150.5(3)
C16–H16···O6	3.534(6)	2.627(5)	165.0(3)
C25–H25···O7	3.361(1)	2.458(9)	162.7(3)

in side cleft binding fashion. However, obvious difference was noticed in anion coordination mode as expected. In complex **4**, seven coordinated NO_3^- anion is surrounded by two cationic receptors and water molecules via one N···H−O, two Ow···H−O and four C···H−O contacts (Fig. 1c). Details inspection reveals that O4 and O6 accept two and one methylene hydrogen H21A, H22B and H11B respectively. O5 of NO_3^- ion is making four contacts *via* one amide hydrogen H4N, one ortho H29 and two water O7w molecules. Notably, the crystalline water molecule act as bridging H-bond donors between two NO_3^- ions thus forming a discrete nitrate-water cluster $[(NO_3^-)_2\text{-}(H_2O)_2]^{4-}$ (Fig. S3a). The anion-water contacts in the cluster are O7w···O5 = 2.770(2) and 2.880(2) Å. The cluster is surrounded by six $\mathbf{L_1H^+}$ and completely encapsulated in the cavity made of these receptors. The other short contacts originating from –CN group is appeared to be is similar to those of the other complexes. The structural aspect of the perchlorate complex **5** is similar to those of the other complexes. The ClO_4^- ion is surrounded by total five cationic tripodal receptors and is coordinated by ten intermolecular H- bonds (Fig. 1d). ClO_4^- ion forms one amide N···H−O, three aromatic C···H−O and six methylene C···H−O contacts reaching a total of ten H-bonds. The oxygen O4 behaves as trifurcated H-bond acceptor from H4N amide NH (N4) and two methylene H21A and H22A. O5 atoms are involved in H-bonding to one aromatic H26 and two methylene hydrogen H11B and H22b. The oxygen O6 offer trifurcated H-bonds and oxygen is connected with one aromatic H16 and two methylene H1A and H11A. O7 is single point H-bonded to aromatic H25. The details of bond distance and angle are given in Table 1.

Second generation tripodal amide L_2 and its anion complexation

The first generation tripodal amide could not encapsulate the anions inside its C_{3v} symmetric cavity, possibly the intramolecular H-bond tightly hold the arms, which resists opening of the cavity to encapsulate anions. Concomitantly the conformation became very rigid and not suitable for guest encapsulation. Keeping mind these possible drawbacks which were great setback in case of $\mathbf{L_1}$, we have decided to enlarge the length of the arm by which the anion binding site shifted to a distant position surely ruled out the close contact between amide NH and CO and clearly generate big space. This design ruled out the possibilities of intramolecular H-bond formation between amide NH and CO and helps to open up the structure to accommodate anionic guests. The real inspiration was the success of anion encapsulated second generation tripodal amide and urea receptors from our group.[32,40] We extended our study to evaluate substitution and cavity effect for anion recognition and synthesized several salts of $\mathbf{L_2}$ with anions of various dimensionality like spherical, planar, tetrahedral and octahedral. Crystallization of the receptor $\mathbf{L_2}$ in neutral medium was unsuccessful unlike $\mathbf{L_1}$.

The bifluoride complex was obtained **[4LH·4HF$_2$·3H$_2$O](6)** from reaction of $\mathbf{L_2}$ with HF in plastic vial. Crystal structure shows significant change in conformation of the receptor in contrast to first generation tripodal $\mathbf{L_1}$, where one arm of the protonated tripodal receptor is directed opposite to the other two arms (Fig. S4a). As expected the anion coordination and other solid state interaction pattern changed dramatically compared to $\mathbf{L_1}$. The apical N-atom is H-bonded with the ethereal oxygen atom (O2 and O3) of two closely connected arms. Very interestingly the arm which is directed opposite to the other two arms is strongly H-bonded with apical NH^+ *via* nitrogen of −CN group forming a pseudo C_{3v} symmetric cavity (Fig. S4b). Very interestingly we have observed the formation of HF_2^- species on treatment with HF acid. Details structural analysis shows that HF_2^- resides around pseudo cavity, F1 ion is strongly H-bonded to one amide hydrogen H2 and three aromatic hydrogen H5, H11 and H29 as depicted in Fig. 2a.

There is no more intramolecular H-bond between amide hydrogen and carbonyl as per our assumption and between two closely connected arms enough space was there that few water molecules had to come and fill up the pseudo cavity through various interactions. The other F2 of HF_2^- also encapsulated in the pseudo cavity and H-bonded with amide hydrogen H7A and two aromatic hydrogen H11 and H46. Stabilization of such kind bifluoride in amide based macrocyclic receptor is also reported by Bowman-James and coworkers.[41] Moreover, a close inspection of the H-bond interaction between carbonyl and CH resulted a dimeric like structure of the receptor where O4 acts as acceptor from H34A and H36. The progress 1D dimeric assembly with help of cyano group through formation of C−H···N and C−H···π contacts is shown in Fig. S4c. The attempt was made to make other halide complexes. However, due to poor crystal quality and corresponding data, chloride and iodide complex can't be reported, but structure of the bromide complex **[L_2H·Br](7)** could be solved with satisfaction. Though roughly we could see from these structure, conformation of the receptor remains same as in complex **6**, only difference is that they contains solvent water or DMF molecules as crystallizing solvent. Very interestingly we noticed that chloride, bromide and iodide complexes are isostructural though complex **6** do not belong to this category. A sharp difference in orientation of one amide hydrogen H3N of two closely connected arms was observed compared to complex **6** and remains outside of the pseudo cavity (Fig. S5a). As a consequence solid states interactions changed noticeably. In case of bromide complex we could not assign the solvent molecules, hence PLATON/SQUEEZE was performed to refine the receptor along with the bromide ion (1.5 Br ion) by excluding the disordered solvent electron densities. This calculated amount of 554 electrons per unit cell or 98 electrons per molecule may be attributed to two water and two DMF molecules which also supported by thermogravimetric analysis (TGA) (Fig. S10) of the crystals. . The distant arm is H-bonded with protonated apical N-atom through cyano group forming a pseudocavity similar to complex **6**. Interaction of Br1 in Fig. 2a shows it is tetra coordinated and all four donor atoms lie on a perfect square geometry. Br1 accept hydrogen from two symmetric amide H3N and methylene H1A. The other half occupied Br2 ion is H-bonded with amide hydrogen H2N and ortho aromatic hydrogen H16. The contacts around bromide ion fall in the range of 3.471(2)-3.808(2) Å. The contacts details are given in Table 3. Close contact between receptors through cyano N7 and methylene hydrogen H33A which connects two layer of pseudo capsular assembly as depicted in Fig. S5b. The contacts around bromide ion fall in the range of 3.471(2)-3.808(2) Å.

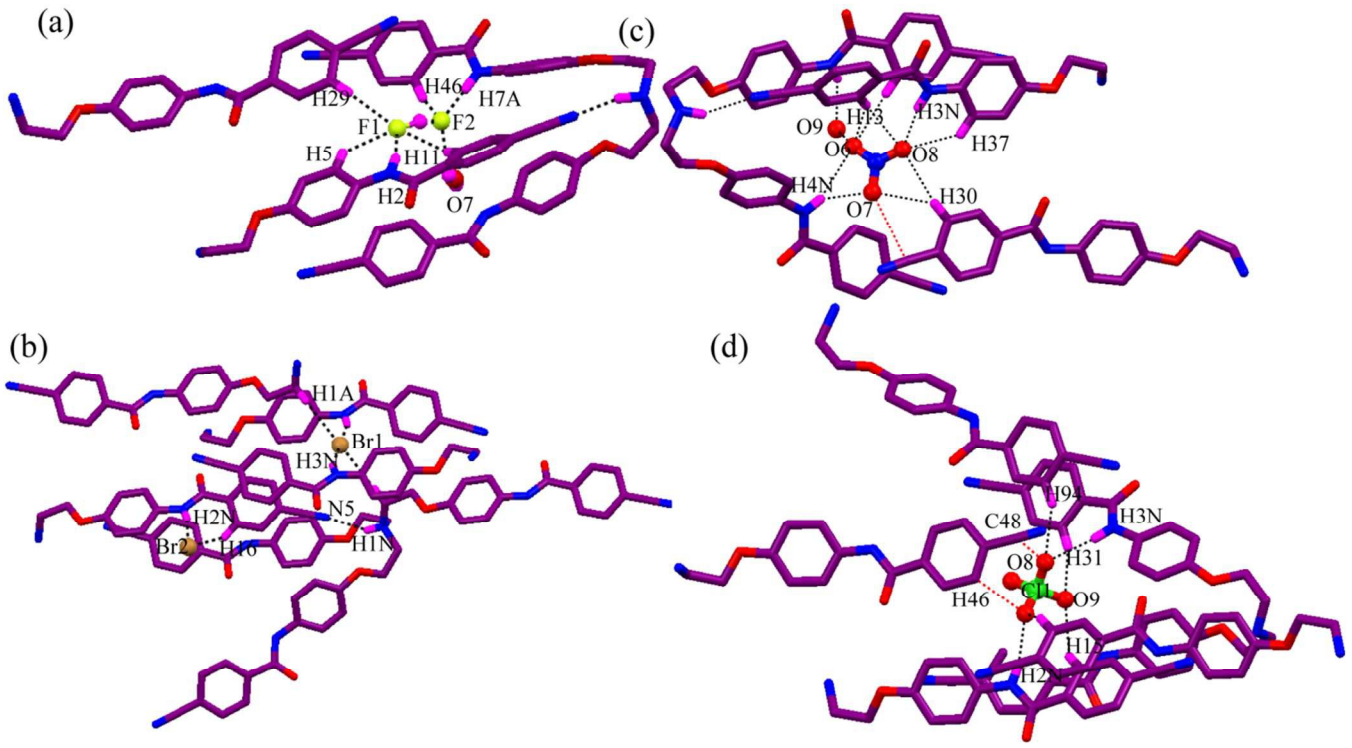

Fig. 2 (a) Crystal structure of complex [**4LH·4HF_2·3H_2O](6)** depicting the interaction of amide hydrogen with HF_2^- and formation of pseudo capsular cavity. (b) Illustration of various H-bonding interactions around bromide in complex **[L_2H·Br](7)**. (c) Illustration of various H-bonding interactions around NO_3^- in complex **[L_2H·NO_3·H_2O](8)**. (d) Partial view of the eight coordinated ClO_4^- ion in complex **[L_2H·ClO_4](9)**. The red contact implies Anion···π interaction (π electron of –CN).

Further receptor-anion interaction was also investigated for planar oxyanion *i.e.* NO_3^- ion by analyzing the crystal structure of the complex **[L_2H·NO_3·H_2O](8)**. The conformation of the receptor is similar to complex **6**. Structural analysis of complex **8** revealed that the distant arm is responsible to from a pseudo capsular cavity, however, unlike bromide complex **7** amide hydrogen of two closely connected arms are pointed towards the cavity. In this case NO_3^- is eleven coordinated arising from

two amide N–H···O, four aromatic C–H···O one water Ow–H···O and one anion···π (π cloud of –CN). The nitrate oxygen O6 is involved in strong H-bond with H4N and O9w, and moderate C–H···O interaction with the aromatic hydrogen H27 and H43 whereas O8 is in interaction with the amide H3N and aromatic H30, H37 and H43 suggesting that each O6 and O8 behaves as tetrafurcated H-bond acceptors in the anion complex. In addition to the above eight interactions, nitrate oxygen O7 is engaged in H-bonding interaction with amide H4N and the aromatic hydrogen H30 including interesting anion···π interaction coming from π enriched –CN group (N5). which include interesting anion···π interaction originating from π enriched –CN group (N5). The nitrate-water cluster $[(NO_3^-)_2$-$H_2O]^{2-}$ is nearly planar and confined within the void created by the receptors (Fig. S6b). The water O9w accepts two amide hydrogen H2N giving tetracoordinated nearly planar geometry. The other water molecule O9Aw shows similar geometry by interacting with methylene hydrogen H2B and carbonyl oxygen O3. One carbonyl oxygen O3 of the folded tripodal arm is H-bonded with aromatic and methylene hydrogen H4 and H2A form a dimeric interaction between two receptors like complex **6**. The dimer is self-organized *via* C–H···O/N (carbonyl and cyano) H-bonds between different aromatic and methylene hydrogen atoms.

The anion complex of the receptor with tetrahedral oxyanion like perchlorate was also prepared. In this case there exists certain amount of DMF-water solvent trapped in the crystal lattice in a disordered manner. These electron densities were moved during refinement and the count of electron removed in total was 226 per two symmetry independent molecules which account for five DMF and three water molecules and further verified by TGA experiment (Fig. S11) of the crystal of complex **9**. Similar mode of conformational adaptability has been found in complex **9**. The perchlorate anion occupies the pseudo cavity generated by three arms of two receptors as showed in Fig. S7a. The symmetrically non-equivalent ClO_4^- ions involving chlorine atoms Cl(1) and Cl(2) are H-bonded with six arms of five tripodal receptors and four arms of three tripodal receptors respectively (Fig. 2d and Fig. S7c). $Cl(1)O_4^-$ and $Cl(2)O_4^-$ ion shows eight and seven coordination respectively. Perchlorate oxygen O8 acts as bifurcated H-bond acceptor with amide and aromatic hydrogen H3N and H94 including one interesting anion···π interaction between $Cl(1)O_4^-$ and π cloud of electron rich –CN group, whereas O9 behaves as bifurcated H-bond acceptor by interacting with two aromatic protons H31 and H15. O10 behaves as trifurcated H-bond by accepting amide and aromatic hydrogen H2N and H12, H15 finally satisfying eight coordination. The details contacts parameters are given in Table 1. The overall non-covalent interactions result in the formation assembly of receptors stitching the adjacent arrays by C–H···O/N (carbonyl and –CN group) H-bonds.

Anion specific conformational adaptability of the second generation tripodal amide

The elongated second generation tripodal receptor $\mathbf{L_2}$ shows a dramatic conformational change in presence of only octahedral SiF_6^{2-} anion in hexafluorosilicate complex $\mathbf{[(L_2H)_2{\cdot}SiF_6{\cdot}4H_2O{\cdot}2DMF](10)}$. The X-ray structure indicates the asymmetric unit contains one mono protonated $\mathbf{L_2H^+}$, one-half hexafluoro silicate anion, two water and one DMF molecule as crystallizing solvent. The intramolecular H-bonding interactions are different than those observed in other complexes of the $\mathbf{L_2}$ receptor. In this case, the *endo* orientated hydrogen is internally bonded with three ethereal oxygen atoms with average N···O distance of 2.70 Å. These H-bonding interactions are responsible for change in conformation of the receptor from open to close orientation (Fig. 3a). This structure is very similar to our previously reported nitro-phenyl appended second generation tripodal amide.[33] Where we had showed solvent induced binding discrepancy of SiF_6^{2-} anion. In other communication we had structurally authenticated for the conformational changes in cresol-based tripodal receptor, based on anion specificity.[27] The C_{2v} symmetric tripodal amide changes to completely folded conformation (C_{3v}) in presence of only SiF_6^{2-} anion and stabilize the anion through formation of a sandwich type complex in side cleft binding mode (Fig. 3b) mainly by mainly N–H···F, Ow–H···F and C–H···F type H-bonds (Fig. 3c). Though all three arms are in same direction, the protonated receptor is not able to create a suitable cavity to encapsulate the anion. Only two arms from each receptor interact with SiF_6^{2-}, while the third arm forms H-bonds with the oxygen atom of a carbonyl group of the next side arm of the same receptor. The binding of SiF_6^{2-} clearly demonstrates that the anion in complex **10** is located outside the tripodal cavity and stabilized by mainly N–H···F and C–H···F H-bonds from the four receptors with addition of Ow–H···F from two water molecules as depicted in Fig. 3c. The other three fluorine atoms are symmetry equivalent, having similar contact point resulting overall in ten H-bonding contacts on SiF_6^{2-} anion. The short contacts around –CN group is quite different than that observed in the other complexes of $\mathbf{L_2}$. π electron cloud none of the –CN group does not participate any contacts unlike the other complex. Only one –CN (N7) group participate in H-bonding with aromatic hydrogen H12, while two are reluctant to form any contacts.

Table 2 Number and nature coordination of anions in $\mathbf{L_1}$ and $\mathbf{L_2}$.

Anions	$\mathbf{L_1}$	$\mathbf{L_2}$
F^-	----	5 (one NH, one OH and three CH)
Br^-	3 (one NH and two CH_2)	4 (two NH and two CH_2)
I^-	3 (one NH and two CH_2)	----
NO_3^-	7 (one NH, two OH, one CH and three CH_2)	11 (two NH, one OH, four CH and one anion···π)
ClO_4^-	10 (one NH, three CH and six CH_2)	8 and 7 (four NH, seven CH, one CH_2 and one anion···π)
SiF_6^{2-}	----	10 (two NH, two OH two CH and four CH_2)

NH = amide, OH = water, CH = aromatic, CH_2 = methylene hydrogen

Table 3 H-bonding contacts in $\mathbf{L_2}$ and its anion complexes.

D–H···A	d(D···A)/ Å	d(H···A)/Å	∠(D–H–A)/º
[4LH·4HF$_2$·3H$_2$O](6)			
N4–H4N···O7	3.41(6)	2.58(1)	163.0(4)
N7–H7A···F2	2.79(1)	2.00(6)	153.0(4)
N2–H2···F1	2.85(7)	2.01(4)	164.0(3)
C5–H5···F1	3.214(7)	2.46(3)	138.0(4)
C11–H11···F1	3.222(7)	2.44(4)	142.0(3)
C29–H29···F1	3.390(1)	2.48(4)	167.0(5)
[$\mathbf{L_2}$H·Br](7)			
N2–H2N···Br2	3.47(2)	2.62(1)	168.0(1)
N3–H2N ···Br1	3.50(2)	2.68(1)	159.0(1)
C1–H1A···Br1	3.81(2)	2.88(1)	160.0(1)
C15–H16···Br2	3.582(3)	2.982(1)	123.7(2)
[$\mathbf{L_2}$H·NO$_3$·H$_2$O](8)			
N4–H4N···O6	2.59(3)	3.37(4)	152.0(2)
O9w···O6	2.887(3)	---	---
C27–H27···O6	3.630(4)	2.716(3)	167.6(2)
C43–H43···O6	3.247(4)	2.457(3)	142.9(2)
C30–H30···O7	2.599(3)	3.345(5)	132.0(2)
N4–H4N···O7	3.01(4)	2.37(3)	138.0(2)
O7···π (anion···π)	3.162(4)	---	---
N3–H3N···O8	2.94(3)	2.11(2)	162.0(2)
C30–H30···O8	3.495(4)	2.589(2)	165.1(2)
C37–H37···O8	3.228(4)	2.470(2)	138.8(2)
C43–H43···O8	3.284(4)	2.504(2)	141.6(2)
[$\mathbf{L_2}$H·ClO$_4$](9)			
N3–H3N···O8	3.36(9)	2.54(7)	159.0(4)
O8···π (anion···π)	3.160(1)	---	---
C94–H94···O8	3.298(8)	2.458(6)	146.4(4)
C15–H15···O9	3.360(7)	2.571(4)	143.0(3)
C31–H31···O9	3.467(8)	2.606(5)	154.2(5)
N2–H2N···O10	3.02(6)	2.18(4)	167.0(3)
C7–H7···O10	3.398(7)	2.605(4)	143.7(3)
C12–H12···O10	3.437(7)	2.650(4)	142.8(4)
C75–H75···O17	3.390(1)	2.470(8)	172.6(4)
N11–H11N···O18	3.01(7)	2.19(6)	160.0(3)
C85–H85···O18	3.348(8)	2.678(6)	129.6(3)
N9–H9N···O20	3.07(6)	2.24(4)	162.0(3)
C53–H53···O20	3.319(7)	2.534(4)	142.3(4)
C59–H59···O20	3.279(7)	2.367(4)	166.4(4)
C66–H66B···O20	3.450(8)	2.498(5)	166.5(3)
[($\mathbf{L_2}$H)$_2$·SIF$_6$·4H$_2$O·2DMF](10)			
N2–H2N···O8w	3.00(6)	2.17(4)	162.0(3)
C17–H17B···F1	3.057(5)	2.231(2)	142.4(3)
O8w···F1	2.875(4)	2.16(8)	145.0(9)
C27–H27···F2	3.380(7)	2.525(3)	153.0(4)
N4–H4N···F3	2.81(4)	2.05(2)	146.0(3)
C1–H1B···F3	3.263(4)	2.369(2)	152.9(3)
N6–H6N···O3	2.98(6)	2.12(4)	174.0(3)

Anion binding studies in solution by 1H NMR spectroscopy

The interesting solid state chemistry of the acidic amide protons also insists us to investigate its solution phase interaction with various guest anions. For this, the respective solution of anions was added sequentially to the DMSO solution of the receptors (DMSO is chosen for the solubility purpose) and the changes in the protons frequencies are recorded at room temperature. The maximum shift is observed for the fluoride among the halides (Cl^-, Br^- and I^-) while it is the dihydrogen phosphate which dominates among the oxyanions like NO_3^- and ClO_4^-. Again between the two amide based receptors, $\mathbf{L_2}$ interacts in an effective way than $\mathbf{L_1}$ as greater shift of NH hydrogen is observed in $\mathbf{L_2}$ (Fig. 4) which is probably due to the presence of more acidic amide NH in this receptor. The amide NH of $\mathbf{L_1}$ is shifted downfield upon addition of fluoride solution while aromatic CHs are splited and moved into opposite directions

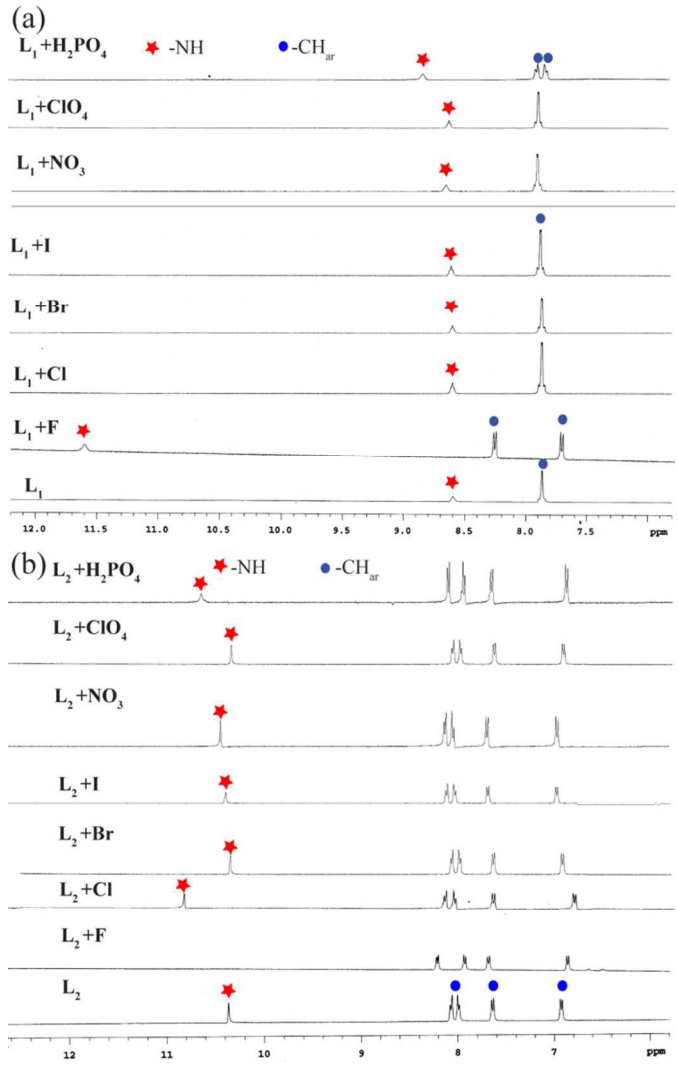

Fig. 4 Partial ^{1}H NMR spectra in DMSO-d_6 showing the maximum observable shifts of amide –NH peak upon the addition of excess (5 equiv.) anions in $\mathbf{L_1}$ and $\mathbf{L_2}$.

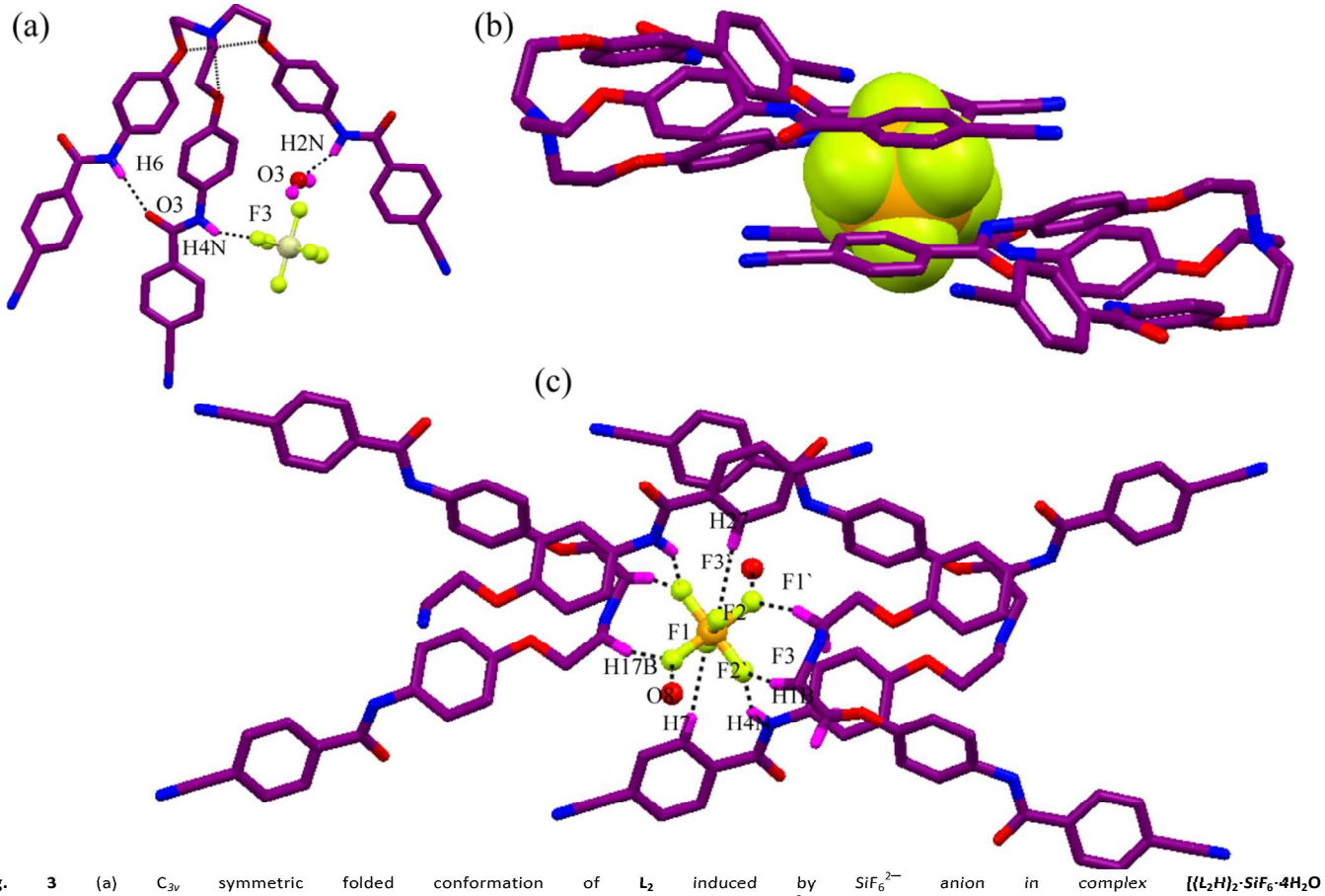

Fig. 3 (a) C_{3v} symmetric folded conformation of L_2 induced by SiF_6^{2-} anion in complex ***[(L₂H)₂·SiF₆·4H₂O ·2DMF](10)***. (b) Sandwich type complex formation in solid state. (c) Coordination environment of SiF_6^{2-} anion.

(Fig. 5a). This could be explained on the basis of two different effects of the hydrogen bonding interactions between the guest anions and the receptor on the aromatic CH: first, the increases in electron density on the aromatic ring through-bond propagation induces a shielding effect; secondly, the increase of polarization of the C–H bonds through space which creates a positive charge on the aromatic hydrogen caused deshielding.[42] Thus, it must be the ortho-CH (CHa), next to the NH which experiences a through space polarization effect and moved to downfield region and as the CH(b) is far away from the amide hydrogen, it experiences a upfield shift due to the through bond charge propagation associated with the hydrogen bonded complex. The strong involvement of the amide NH is reflected in the ppm vs equv plot (Fig. 6a) which recorded a huge downfield shift of 3.014 ppm after 8 equv. of fluoride solution. At this stage, CHa is shifted to 0.43 downfield and CHb to 0.117 upfield. Another basic anion $H_2PO_4^-$, however interacts weakly with the receptor $\mathbf{L_1}$ and after 3 equv. of the aforesaid anion, the NHa is shifted 0.183 ppm downfield. Again, the changes with the anions such as Cl^-, Br^-, NO_3^- etc are negligible (Fig. S38-S40).

Deprotonation of NH protons is observed for $\mathbf{L_2}$ in presence of fluoride anion. However as shown in Fig. 5b, all other aromatic CHs are also on moved with the escalating the concentration of the aforesaid anion solution. The H_b and H_c are shifted downfield (Δ ppm Hb = 0.028, Δ ppm Hc = 0.126) while H_a and H_d (Δ ppm Ha = 0.073, Δ ppm Hd = 0.08) which are far away from the amide NH are shifted upfield. Thus the first set of protons which are pointed in the same direction of the amide NH are definitely polarized through space interaction by the guest fluoride anion and that is why they are shifted to downfield. And due to the formation of the same negatively charged species the second set of protons are upfield shifted. first set of protons which are pointed in the same direction of the amide NH are definitely polarized through space interaction However, after excess addition of fluoride we also did not observe the characteristic HF_2^- peak at downfield region. This is probably due to the lower stability of the HF_2^- species in the solution.[43] Again with $H_2PO_4^-$ anion, the NH_a is shifted to 0.276 ppm downfield and the aromatic CHs interacts in the same fashion (Δ ppm H_a = -0.034, Δ ppm H_b = 0.026, Δ ppm H_c =0.039 and Δ ppm H_d = -0.027). Again, the changes with the anions such as Cl^-, Br^-, NO_3^- etc are negligible (Fig. S41-S43).

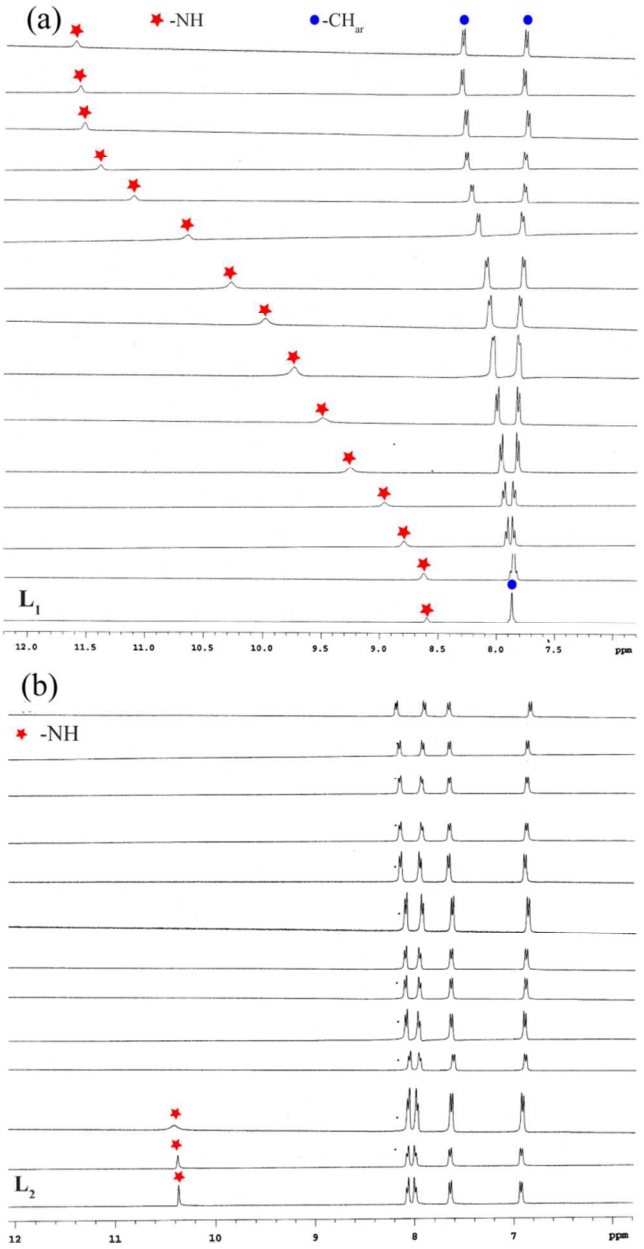

Fig. 5 Stacking plot showing shift of amide –NH and –CH hydrogen with gradual addition of TBAF solution to $\mathbf{L_1}$ and $\mathbf{L_2}$ in DMSO-d_6.

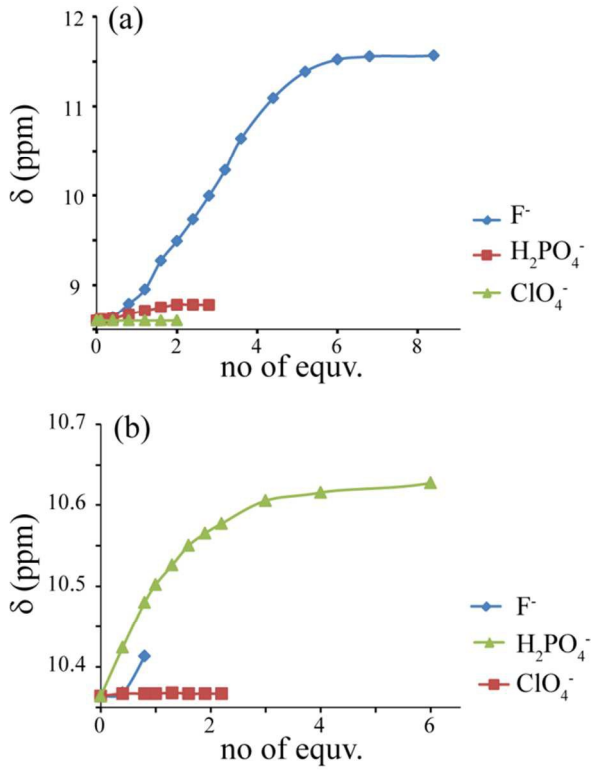

Fig. 6 (a) and (b) ^{1}H NMR titration curves of $\mathbf{L_1}$ and $\mathbf{L_2}$ with anions in DMSO-d_6 at RT. Net changes in the chemical shifts of amidic –NH is shown against the increasing amount anions.

Conclusions

In summary, we have synthesized cyanobenzoyl substituted two tripodal amide receptors of having different length and successfully exploited their high potential towards anion recognition of various dimensionalities. The C_{3v} symmetric first generation tripodal $\mathbf{L_1}$ remains as locked conformation in free and protonated states through intramolecular N–H···O H-bond. This incur encapsulation of anions irrespective of size, shape and charge, therefore anion recognition take place through side cleft binding fashion only. Then we have applied a synthesis stagey to cancel intramolecular H-bond, where cyanobenzoyl was appended from a bigger platform like triphenyl amine to give second generation tripodal $\mathbf{L_2}$. Such modification resulted three major advantages like (i) the possibility of making C_{3v} symmetric cavity for anion encapsulation as the H-bonding between apical N-atom and ethereal O-atom could be able to hold three arms tightly, (ii) ruled out the intramolecular N–H···O H-bond which make amide hydrogen ready for anions and (iii) produced larger space for anion recognition. Though the crystal structure of the anion complexes shows close vicinity of two arms, while the other projected in the opposite direction. In the protonated state one arm is H-bonded with apical N-atom through –CN group forming pseudo capsular cavity. The anions remain in the pseudo cavity and H-bonded with one or more amide hydrogen. The most appealing feature of the $\mathbf{L_2}$ is that selective anion induced reorganization resulted change in conformation from open C_{2v} symmetry to folded C_{3v} in presence of only SiF_6^{2-} anion and forms a sandwich type complex. Two neutral receptors interacts with fluoride ion strongly among the halide ions as very large chemical shift of amide hydrogen observed. Though the receptors are reluctant to bind with oxyanion strongly except relatively better amide hydrogen shift by $H_2PO_4^-$ in both receptors. It is also clear form solution studies that anion interacts with $\mathbf{L_2}$ to a greater extent than $\mathbf{L_1}$. This phenomena is further validated by its solid state anion binding as the number of H-bond around anions in $\mathbf{L_2}$ is apparently higher than in $\mathbf{L_1}$.

EXPERIMENTAL

Materials and method

All reagents were obtained from commercial sources and used as received. Solvents were distilled freshly following standard procedures. Tris(2-aminoethyl)amine (tren), triethanol amine and 4-cyanobenzoyl chloride were purchased from Sigma-Aldrich and used as received. Solvents for synthesis and crystallization experiments were purchased from Merck, India, and used as received.

Instrument

IR spectra were recorded on a Perkin-Elmer-Spectrum One FT-IR spectrometer with KBr disks in the range 4000–500 cm^{-1} NMR spectra were recorded on a Varian FT-400/600 MHz instrument. Chemical shifts were recorded in parts per million (ppm) on the scale solvent peak as reference. ESI-MS spectra were recorded in a WATERS LC-MS/MS system, Q-Tof Premier in the Central Instrument Facility (CIF) of IIT Guwahati. The thermal analyses were performed by using an SDTA 851 e TGA thermal analyzer (Mettler Toledo) with a heating rate of 5 °C per min in a N_2 atmosphere.

Crystallographic refinement details

The crystallographic data and details of the data collection for free receptor **L_1(1)** and anion complexes **2**, **3**, **4**, **5**, **6**, **7**, **8**, **9** and **10** are given in Table S1. In each case, a crystal of suitable size was selected from the mother liquor and immersed into silicone oil, then mounted on the tip of a glass fiber and cemented using epoxy resin. Intensity data for the all crystals were collected Mo-K_α radiation (λ = 0.71073Å) at 298(2) K, with increasing ω (width of 0.3° per frame) at a scan speed of 6 s/ frame on a Bruker SMART APEX diffractometer equipped with CCD area detector. The data integration and reduction were processed with SAINT[44] software. An empirical absorption correction was applied to the collected reflections with SADABS.[45] The structures were solved by direct methods using SHELXTL[46] and were refined on F^2 by the full-matrix least-squares technique using the SHELXL-97 program package.[47] Graphics are generated using MERCURY 3.0.[48] In all cases, non-hydrogen atoms are treated anisotropically. Wherever possible, the hydrogen atoms are located on a difference Fourier map and refined. In other cases, the hydrogen atoms are geometrically fixed. PLATON/SQUEEZE[49] was performed to refine the host framework in **7** and **9** excluding the disordered solvent electron densities and the details calculations are explained in respective structure discussion section. These crystallographic calculations were further conformed by TGA experiment (ESI).

NMR studies

^{1}H NMR titration studies were done to evaluate the interaction of **L_1** and **L_2** with anions in DMSO-d_6 at room temperature. Initial concentrations were $[ligand]_0$ = 5 mM, and $[anion]_0$ = 50 mM. Each titration was performed by 10–12 measurements at room temperature.

Synthesis and characterization

First generation tripodal amide L_1: Tripodal amide-based receptor **L_1** was synthesized by the reaction of tris(2-aminoethyl)amine with three equivalents of 4-cyanobenzoyl chloride in presence of triethylamine in dry CH_2Cl_2 at 0 °C.[23] After stirring for 8 hrs the reaction mixture was filtered off and the precipitate was washed with plenty of water and methanol to remove the triethylammonium chloride and dried under vacuum to yield the colorless solid of **L_1** (Yield = 86%). Block shaped crystals of **L_1** were grown from DMF solution (Scheme S2).

Compound L_1(1): Yield = 80%, M. P: >300 °C. ^{1}H-NMR (600 MHz, DMSO-d_6) δ (ppm): 8.712 (br, 3H, NH), 7.951 (d, 6H, ArH, J = 7. 0 Hz), 7.942 (d, 6H, ArH, J = 7.0 Hz), 3.33 (m, 6H, NCH_2), 2.81 (m, 6H, $NHCH_2CH_2$). ^{1}H-NMR (150 MHz, DMSO-d_6): 164.98, 138.36, 132.30, 127.92, 118.28, 113.47, 52.96 and 37.2. IR spectra (KBr pellet): 3277 cm^{-1} *vs*(N–H), 2983 cm^{-1} *vs*(C–H), 2824 cm^{-1} (C–H), 2228 *vs*(C≡N), 1640 *vs*(CO), 1538 cm^{-1} *vs*(C=C). ESI mass [M+1] m/z = 534.2230 (calcd 534.590)

***Second generation tripodal amide* L_2**: Receptor **L_2** was synthesized by following reported procedure.[30-33] The nitro tripodal (B) was obtained from the treatment of tris(2-chloroethyl)amine hydrochloride[50] (A) by SN^2 substitution with 4-nitrophenol in EtOH (Yield 65%) followed by reduction of nitro group to yield corresponding triamine (C) (Yield 72%). Subsequently, triamine (C) solution in CH_2Cl_2 was slowly added to a mixture of three equivalents of 4-cyanobenzoyl chloride in presence of triethylamine in dry CH_2Cl_2 and stirred for 8 hrs at 0 °C. The reaction mixture is filtered off and the precipitate is washed with water and methanol to remove the triethylammonium chloride and dried under vacuum to yield the gray solid of **L_2** (Yield = 80%). See scheme S1 and S2 for detailed synthesis.

Compound L_2: Yield = 85%, M. P: 175-177 °C. ^{1}H-NMR (600 MHz, DMSO-d_6) δ (ppm): 10.364 (s, 3N–H), 8.079 (d, 6H, ArH, J = 7.1 Hz), 8.004(d, 6H, ArH, J = 7.3 Hz), 7.654 (d, 6H, ArH, J = 7.0 Hz), 6.940 (d, 6H, ArH, J = 7.2 Hz), 4.087 (t, 6H, -OCH_2, J = 5.4) and 3.05 (t, 6H, -NCH_2, J = 5.8). ^{13}C-NMR (150 MHz, DMSO-d_6): 163.73, 155.08, 149.27, 139.07, 132.47, 131.87, 128.47, 122.14, 118.40, 115.56, 114.57, 113.73, 66.51 and 53.71. IR spectra (KBr pellet): 3287cm^{-1} *vs*(N–H), 3074 cm^{-1} *vs*(C–H), 2870 cm^{-1} (C–H), 2240 *vs*(C≡N), 1640 *vs*(CO), 1515 cm^{-1} *vs*(C=C). ESI mass [M+1] m/z = 810.3070 (calcd. 810.870).

Preparation of anion complex of the receptors L_1 and L_2

All Complexes were obtained by stirring L_1 or L_2 (0.05 mM) in 5 mL of DMF in a glass beaker (or plastic vial for complex 6) and 1.2 equiv. of corresponding acid like 40% HF, 49% HBr, 55% HI, HNO_3 and 70% $HClO_4$. After a constant stirring for half an hour, the clear solution was allowed to slow evaporation. Single crystals suitable for X-ray diffraction analysis were obtained at RT within 2–3 weeks.

[L_1H·Br](2): Yield = 75%, M. P: >300 °C. ^{1}H-NMR (600 MHz, DMSO-d_6) δ (ppm): 8.995 (br, 3H, NH), 7.939 (d, 6H,

ArH, J = 6.8 Hz), 7.889 (d, 6H, ArH, J = 7.1 Hz) 3.733 (m, 6H, NCH_2), 3.419 (m, 6H, $NHCH_2CH_2$). IR spectra (KBr pellet): 3342 cm^{-1} *vs*(N–H), 2983 cm^{-1} *vs*(C–H), 2824 cm^{-1} (C–H), 2231 *vs*(C≡N), 1648 *vs*(CO), 1541 cm^{-1} *vs*(C=C).

[L_1H·I](3): Yield = 70%, M. P: >300 °C. ^{1}H-NMR (600 MHz, DMSO-d_6) δ (ppm): 8.992 (br, 3H, NH), 7.935 (d, 6H, ArH, J = 6.9 Hz), 7.882 (d, 6H, ArH, J = 7.0 Hz) 3.730 (m, 6H, NCH_2), 3.413 (m, 6H, $NHCH_2CH_2$). IR spectra (KBr pellet): 3277 cm^{-1} *vs*(N–H), 2983 cm^{-1} *vs*(C–H), 2824 cm^{-1} (C–H), 2231 *vs*(C≡N), 1640 *vs*(CO), 1538 cm^{-1} *vs*(C=C).

[L_1H·NO_3]$_2$·H_2O(4): Yield = 65%, M. P: >300 °C. ^{1}H-NMR (600 MHz, DMSO-d_6) δ (ppm): 8.990 (br, 3H, NH), 7.933 (d, 6H, ArH, J = 6.8 Hz), 7.884 (d, 6H, ArH, J = 7.1 Hz) 3.728 (m, 6H, NCH_2), 3.409 (m, 6H, $NHCH_2CH_2$). IR spectra (KBr pellet): 3342 cm^{-1} *vs*(N–H), 3014 cm^{-1} *vs*(C–H), 2901 cm^{-1} (C–H), 2231 *vs*(C≡N), 1648 *vs*(C=O), 1537 cm^{-1} *vs*(C=C), 1379 cm^{-1} *vs*(N=O).

[L_1H·ClO_4](5): Yield = 65%, M. P: >300 °C. ^{1}H-NMR (600 MHz, DMSO-d_6) δ (ppm): 8.990 (br, 3H, NH), 7.930 (d, 6H, ArH, J = 6.9 Hz), 7.883 (d, 6H, ArH, J = 7.0 Hz) 3.725 (m, 6H, NCH_2), 3.406 (m, 6H, $NHCH_2CH_2$). IR spectra (KBr pellet): 3350 cm^{-1} *vs*(N–H), 3046 cm^{-1} *vs*(C–H), 2901 cm^{-1} (C–H), 2231 *vs*(C≡N), 1646 *vs*(C=O), 1537 cm^{-1} *vs*(C=C), 1324 and 1287 cm^{-1} (Cl=O).

[4LH·4HF_2·3H_2O](6): Yield = 65%, M. P: 180-181 °C. ^{1}H-NMR (600 MHz, DMSO-d_6) δ (ppm): 10.383 (s, 3N–H), 8.080 (d, 6H, ArH, J = 6.9 Hz,), 8.010 (d, 6H, ArH, J = 7.0 Hz,), 7.669 (d, 6H, ArH J = 6.8 Hz), 6.961 (d, 6H, ArH, J = 7.1 Hz,), 4.387 (t, 6H, -OCH_2, J = 5.3) and 3.810 (t, 6H, -NCH_2, J = 5.5). IR spectra (KBr pellet): broad band at 3425 *vs*(O–H and N–H), 3083 cm^{-1} *vs*(C–H), 2910 cm^{-1} (C–H), 2231 *vs*(C≡N), 1648 *vs*(CO), 1518 cm^{-1} *vs*(C=C).

[L_2H·Br](7): Yield = 70%, M. P: 195-196 °C. ^{1}H-NMR (600 MHz, DMSO-d_6) δ (ppm): 10.397 (s, 3N–H), 8.083 (d, 6H, ArH, J = 7.0 Hz), 8.011 (d, 6H, ArH, J = 7.2 Hz,), 7.945 (s, DMF solvent) 7.701 (d, 6H, ArH, J = 6.8 Hz), 6.961 (d, 6H, ArH, J = 7.1 Hz,), 4.389 (t, 6H, -OCH_2, J = 5.3) and 3.821 (t, 6H, -NCH_2, J = 5.5) 2.886 (s, DMF solvent) and 2.727 (s, DMF solvent). IR spectra (KBr pellet): broad band at 3425 *vs*(O–H and N–H), 3083 cm^{-1} *vs*(C–H), 2910 cm^{-1} (C–H), 2231 *vs*(C≡N), 1648 *vs*(CO), 1518 cm^{-1} *vs*(C=C).

[L_2H·NO_3·H_2O](8): Yield = 65%, M. P: 205-207 °C. ^{1}H-NMR (600 MHz, DMSO-d_6) δ (ppm): 10.395 (s, 3N–H), 8.080 (d, 6H, ArH, J = 7.3 Hz,), 8.009 (d, 6H, ArH, J = 7.0 Hz,), 7.705 (d, 6H, ArH, J = 6.5 Hz), 6.966 (d, 6H, ArH, J = 7.3 Hz,), 4.383 (t, -OCH_2, J = 5.3 6H) and 3.819 (t, 6H, -NCH_2, J = 5.5). IR spectra (KBr pellet): broad band at 3435 *vs*(O–H and N–H), 2983 cm^{-1} *vs*(C–H), 2910 cm^{-1} (C–H), 2230 *vs*(C≡N), 1657 *vs*(CO), 1528 cm^{-1} *vs*(C=C), 1380 cm^{-1} *vs*(N=O).

[L_2H·ClO_4](9): Yield = 70%, M. P: 211-212 °C. ^{1}H-NMR (600 MHz, DMSO-d_6) δ (ppm): 10.396 (s, 3N–H), 8.082 (d, 6H, ArH, J = 7.0 Hz,), 8.010 (d, 6H, ArH, J = 7.1 Hz), 7.946 (s, DMF solvent) 7.699 (d, 6H, ArH, J = 6.9 Hz), 7.00 (d, 6H, ArH, J = 7.0 Hz,), 4.421 (t, -OCH_2, J = 5.3 6H,) and 3.816 (t, -NCH_2, J = 5.5 6H) 2.885 (s, DMF solvent) and 2.726 (s, DMF solvent). IR spectra (KBr pellet): broad band at 3435 *vs*(O–H and N–H), 3093 cm^{-1} *vs*(C–H), 2962 cm^{-1} (C–H), 2230 *vs*(C≡N), 1657 *vs*(CO), 1520 cm^{-1} *vs*(C=C) 1259 and 1240 cm^{-1} (Cl=O).

[(L_2H)$_2$·SIF_6·4H_2O·2DMF](10): Yield = 60%, M. P: 229-230 °C. ^{1}H-NMR (600 MHz, DMSO-d_6) δ (ppm): 10.397 (s, 3N–H), 8.084 (d, 6H, ArH, J = 7.3 Hz), 8.013 (d, 6H, ArH, J = 7.0 Hz), 7.945 (s, DMF solvent) 7.701(d, 6H, ArH, J = 6.8 Hz), 7.01 (d, 6H, ArH, J = 7.0 Hz,), 4.396 (t, 6H, -OCH_2, J = 5.5) and 3.814 (t, 6H, -NCH_2, J = 5.6) 2.884 (s, DMF solvent) and 2.725 (s, DMF solvent). IR spectra (KBr pellet): broad band at 3440 *vs*(O–H and N–H), 3120 cm^{-1} *vs*(C–H), 2963 cm^{-1} (C–H), 2222 *vs*(C≡N), 1656 *vs*(CO), 1518 cm^{-1} *vs*(C=C).

Acknowledgements

This work was supported by CSIR and SERB through grant 01-2235/08/EMR-II and SR/S1/OC-62/2011, New Delhi, India. CIF IITG and DST-FIST for providing instrument facilities. N.H thanks IITG for fellowship.

Notes and references

Department of Chemistry, Indian Institute of Technology Guwahati, Assam-781039
Fax: +91-361-2582349; Tel: +91-361-2582313; E-mail: gdas@iitg.ernet.in.

†Electronic Supplementary Information (ESI) available: synthetic scheme of **L_1** and **L_2**, X-ray crystal structures for all complexes, TGA, IR, NMR and Mass spectra of the complexes and NMR titration plots. See DOI: 10.1039/b000000x/

References

1 S. Ayoob and A. K. Gupta, *Crit. Rev. Environ. Sci. Technol*., 2006, **36**, 433.
2 USEPA, *Perchlorate environmental contamination: Toxicological review and risk characterization*. External review draft. NCEA-1-0503, Washington, DC, 2002.
3 J. L. Sessler, P. A. Gale and W.-S. Cho, *Anion Receptor Chemistry*, Cambridge, 2006.
4 P. A. Gale, S. E. García-Garrido and J. Garric, *Chem. Soc. Rev*., 2008, **37**, 151.
5 R. J. Götz, A. Robertazzi, I. Mutikainen, U. Turpeinen, P. Gamez and J. Reedijk, *Chem. Commun*., 2008, 3384.
6 K. Bowman-James, *Acc. Chem. Res*., 2005, **38**, 671.
7 L. E. Santos-Figueroa, M. E. Moragues, E. Climent, A. Agostini, R. Martínez-Máñez and F. Sancenón, *Chem. Soc. Rev*., 2013, **42**, 3489.
8 D. Rais, J. Yau, D. M. P. Mingos, R. Vilar, A. J. P. White and D. J. Williams, *Angew. Chem., Int. Ed*., 2001, **40**, 3464.
9 N. Gimeno and R. Vilar, *Coord. Chem. Rev*., 2006, **250**, 3161.
10 M. A. Hossain, J. A. Liljegren, D. Powell and K. Bowman-James, *Inorg. Chem.*, 2004, **43**, 3751.
11 P. S. Lakshminarayanan, E. Suresh and P. Ghosh, *Inorg. Chem.*, 2004, **45**, 4372.
12 S. O. Kang, M. A. Hossain, D. Powell and K. Bowman-James, *Chem. Commun*., 2005, 328.
13 M. A. Saeed, J. J. Thompson, F. R. Fronczek and M. A. Hossain, *CrystEngComm*., 2010, **12**, 674.
14 S. K. Dey, B. Ojha and G. Das, *CrystEngComm*., 2011, **13**, 269.

15 Y. Ding, Y. Tang, W. Zhu and Y. Xie, *Chem. Soc. Rev*., 2015, **44**, 1101.
16 B. Chen, Y. Ding, X. Li, W. Zhu, J. P. Hill, K. Ariga and Y. Xie, *Chem. Commun*., 2013, **49**, 10136.
17 Y. Xie, Y. Ding, X. Li, C. Wang, J. P. Hill, K. Ariga, W. Zhanga and W. Zhu, *Chem. Commun*., 2012, **48**, 11513.
18 Y. Ding, T. Li, W. Zhu and Y. Xie *Org. Biomol. Chem*., 2012, **10**, 4201.
19 Q. Wang, Y. Xie, Y. Ding, X. Lia and W. Zhu, *Chem. Commun.*, 2010, **46**, 3669.
20 R. Dutta and P. Ghosh, *Chem. Commun*., 2014, **50**, 10538.
21 J. M. Llinares, D. Powell and K. Bowman-James, *Coord. Chem. Rev*., 2014, **240**, 57.
22 B. L. Schottel, H. T. Chifotides and K. R. Dunbar*, Chem. Soc. Rev*., 2008, **37**, 68.
23 E. Garcia-Espana, P. Díaz, J. M. Llinares and A. Bianchi, *Coord. Chem. Rev*., 2006, **250**, 2952.
24 I. Ravikumar, P.S. Lakshminarayanan and P. Ghosh, *Inorganica Chimica Acta*., 2010, **363**, 2886.
25 J. M. Lehn, *Supramolecular Chemistry Concepts and Perspectives*, VCH, Weinheim, 1995.
26 M. Arunachalam and P. Ghosh, *Chem. Commun*., 2011, **47**, 6269.
27 S. K. Dey, A. Pramanik and G. Das, *CrystEngComm*., 2011, **13**, 1664.
28 S. K. Dey and G. Das, *Chem. Commun*., 2011, **47**, 4983.
29 S. K. Dey, B. K. Dutta and G. Das, *CrystEngComm*., 2012, **14**, 5305.
30 M. N. Hoque and G. Das, *Cryst. Growth Des.*, 2014, **14**, 296.
31 M. N. Hoque and G. Das, *CrystEngComm*., 2014, **16**, 4447.
32 A. Basu and G. Das, *Chem. Commun*., 2013, **49**, 3997.
33 A. Basu, R. Chutia and G. Das, *CrystEngComm*., 2014, **16**, 4886.
34 M. N. Hoque, A. Basu and G. Das, *Cryst. Growth Des*., 2012, **12**, 2153.
35 M. N. Hoque, A. Basu and G. Das, *Supramol. Chem*., 2014, **26**, 392.
36 M. N. Hoque, A. Basu and G. Das, *Cryst. Growth Des*., 2014, **14**, 6.
37 S. K. Dey and G. Das, *Dalton Trans*., 2011, **40**, 12048.
38 A. Basu and G. Das, *Dalton Trans*., 2012, **41**, 10792.
39 S. K. Dey and G. Das, *Dalton Trans*., 2012, **41**, 8960.
40 A. Basu and G. Das, *J. Org. Chem*., 2014, **79**, 2647.
41 S. O. Kang, D. R. Powell, V. W. Day and K. Bowman-James, *Angew. Chem. Int. Ed.,* 2006*,* **45***,* 1921.
42 F. Han, Y. Bao, Z. Yang, T. M. Fyles, J. Zhao, X. Peng, J. Fan, Y. Wu and S. Sun, *Chem. – Eur. J*., 2007, **13**, 2880.
43 D. E. Gómez, L. Fabbrizzi, M. Licchelli and E Monzani, *Org. Biomol. Chem*., 2005, **3**, 1495.
44 G. M. Sheldrick, SAINT and XPREP, 5.1 ed., Siemens Industrial Automation Inc., Madison, WI, 1995.
45 SADABS, empirical absorption Correction Program, University of Göttingen, Göttingen, Germany, 1997.
46 G. M. Sheldrick, SHELXTL Reference Manual: Version 5.1, Bruker AXS, Madison, WI, 1997.
47 G. M. Sheldrick, SHELXL-97: Program for Crystal Structure Refinement, University of Göttingen, Göttingen, Germany, 1997.
48 Mercury 2.3 Supplied with Cambridge Structural Database, CCDC, Cambridge, U.K., 2011–2012.
49 P. Van der Sluis and A. L. Spek, *Acta Crystallogr., Sect. A*: *Found. Crystallogr*., 1990, **46**, 194.
50 Jr. K. Ward, *J. Am. Chem. Soc*., 1935, **57**, 914.

Graphical Abstract

Solid and solution state anion binding *via* side cleft and pseudocapsular fashion by two cyanophenyl substituted first (**L_1**) and second (**L_2**) generation tripodal amide has been demonstrated along with selective anion induced conformational change of **L_2** from open C_{2v} to folded C_{3v} symmetry.